České vysoké učení technické v Praze
Fakulta jaderná a fyzikálně inženýrská

Katedra fyziky
Obor: Fyzika a technika termojaderné fúze

Ubíhající elektrony na tokamacích Compass a Golem

Runaway electrons on the COMPASS and GOLEM tokamaks

RESEARCH TASK

Author: Ondřej Ficker
Supervisor: Doc. RNDr. Jan Mlynář, Ph.D.
Consultant: Ing. Vojtěch Svoboda, CSc.
Year: 2014

Název práce:
Ubíhající elektrony na tokamacích Compass a Golem

Autor: Ondřej Ficker

Obor: Fyzika a technika termojaderné fúze
Druh práce: Výzkumný úkol

Vedoucí práce: Doc. RNDr. Jan Mlynář, Ph.D.
Ústav fyziky plazmatu AV ČR

Konzultant: Ing. Vojtěch Svoboda, CSc.
FJFI ČVUT v Praze

Abstrakt: Ubíhající elektrony představují jedno z největších nebezpečí pro velké termojaderné reaktory. Soustředěný svazek těchto vysokoenergetických elektronů může způsobit závažné poškození materiálu první stěny i dalších komponent. Tato práce obsahuje stručný úvod do problematiky ubíhajících elektronů, popis diagnostických metod a nejdůležitějších poznatků z předchozích experimentů. V praktické části jsou popsány některé výsledky z měření ubíhajících elektronů na tokamakích Compass a Golem. K nejzajímavějším pozorovaným jevům patří vyvrhování elektronů při pilové nestabilitě

Klíčová slova: ubíhající elektrony, tokamak, diagnostika plazmatu

Title:
Runaway electrons on the COMPASS and GOLEM tokamaks

Author: Ondřej Ficker

Abstract: Runaway electrons represent one of the most dangerous issues in the large thermonuclear reactor. The collimated beam of these high energy particles may cause serious damage to the first wall and other components. This work contains brief introduction to the theory of runaway electrons, description of the diagnostic methods and the most important results of previous experiments. In the experimental part, the interesting results of the measurements on the Compass and Golem tokamaks are described. On of the most interesting phenomena is the release of runaway electrons during the saw-teeth instability.

Key words: runaway electrons, tokamak, plasma diagnostics, saw-teeth instability

Contents

Introduction

Thermonuclear fusion is currently the most promising way how to reach practically limitless, clean and once perhaps economically viable source of energy. Such source would be necessary in human desire for progress, comfort and conquest of the Universe.

The achieving of this goal is a long track. It is the goal worth many generations of researchers but we still hope, that our generation will see positive results of expensive research program. Many ways for reaching this goal have been tried, some of them were successful, some of them were discredited. Some of the ways have survived as scientifically interesting. When the time has come to decide which type of a fusion device could offer the fastest way of achieving the Goal, tokamaks were chosen for their reasonable confinement time, relatively simple construction and long history of the research.

All these years of research and experiments were put into the huge project, called International Thermonuclear Experimental Reactor ITER. ITER will prove, whether we can succeed in controlling the fusion and using it for the electricity generation in the near future. In Latin, ITER means the way, the journey or the march. The device itself couldn't get a better name, it is indeed a way we have to undergo if we want to find out more. In the current fusion devices, e. g. JET, we can't simulate conditions of self-sustained burning plasma (the plasma that is effectively heated by alpha particles originating from fusion reactions). Such plasma could behave different from what we know up to now. Will this state of plasma enrich or suppress instabilities? Are our estimates of the confinement time right? ITER has the potential answer to many questions.

One of the problems with an urgent need of solution is the generation and suppression of runaway electrons (RE) in tokamaks. These extremely energetic particles could cause severe damage to the first wall and exposed plasma diagnostics. They can occur in smaller tokamaks but the magnitude of their destructing power will be much larger in ITER.

This research report begins with the brief introduction to the physics behind the runway electrons phenomena, important equations are shortly discussed with references to important papers. These relations or their variations will be derived or examined in detail in subsequent diploma thesis. The theory is followed by a summary of experiments conducted on tokamaks around the world and short description of main modelling tools. The main aim of this work is evaluation of first experiments dedicated to RE on tokamak COMPASS and the data analysis of older shots with RE presence on COMPASS and GOLEM tokamak.

Chapter 1

Runaway Electrons Physics

Fusion plasma in the tokamak consist almost exclusively of charged particles, e.g. electrons, deuterium, tritium, helium and heavier nuclei and ions in various ionisation states. The charged particles are strongly influenced by external fields and fields of other particles. Therefore, the plasma is complex system which behaves collectively. Furthermore, in every macroscopic volume the amount of positive and negative charge is approximately the same, which means the plasma is quasi-neutral.

1.1 Motion of test particle in external field

In external constant electromagnetic field charged particle obeys simple equation of motion with the Lorenz force on the right-hand side

$$m\frac{\mathrm{d}\mathbf{v}}{\mathrm{d}t} = e(\mathbf{E} + \mathbf{v} \times \mathbf{B}). \tag{1.1}$$

Magnetic field $\mathbf{B}$ causes the motion of the particle around magnetic field line (perpendicular to direction of magnetic induction vector) and electric field $\mathbf{E}$ causes acceleration in the parallel direction .

In the tokamak, there are present numerous sources of electric fields and magnetic fields. Toroidal and poloidal electric fields are the strongest magnetic fields, which are generated by external coils and the plasma current. These two components together form a helical topology of magnetic field lines. Particles gyrate around these lines and move along them in both directions, the direction of the plasma current slightly dominates for ions and the other direction for electrons.
The most important component of the electric field in the tokamak is the component in the toroidal direction which is generated by magnetic field of central solenoid. This component is necessary for the tokamak discharge start-up phase and it is the dominant force that drives the current in plasma in early states of the discharge in every tokamak.
Other macroscopic electric fields can be caused by some drift motion, different for positively and negatively charged particles.
To discover the motion of the particle in time-dependent and space-dependent fields

the gyro-centered approach is quite useful. The known gyration around the field line is omitted in this approach, so that the more complex motion of the center of gyration, e.g. drifts, can be studied directly. This approach leads to the equation[11]

$$m\ddot{\mathbf{R}} = \mathbf{F}_{ext} + Q\dot{\mathbf{R}} \times \mathbf{B} - \mu \nabla B, \tag{1.2}$$

where $\mu = \frac{mv_\perp}{2B}$ is the magnetic dipole moment (adiabatic invariant of gyration). The equation (1.2) contains all the information about the motion of the virtual (gyro-centered) particle.

1.1.1 Motion parallel to the magnetic field

If one wants to separate the motion parallel to the magnetic field (this is important when acceleration is considered), the scalar product of the equation (1.2) with the direction of the field $\mathbf{e_B} = \frac{\mathbf{B}}{|\mathbf{B}|}$ gives the relation

$$m\ddot{\mathbf{R}}_\parallel = \mathbf{F}_{ext,\parallel} - \mu(\nabla B)_\parallel. \tag{1.3}$$

The first term on the right-hand side of the equation (1.3) is the component of an external force parallel to the direction of the magnetic field. In a tokamak the force is usually an electric force $\mathbf{F}_e = e\mathbf{E}$. The second term is related to the change of the magnitude of the magnetic field in space. Particularly, only parallel gradients are of importance in the equation (1.3). A non-zero parallel gradient means that the magnetic field lines are getting closer to each other. These gradients cause the effect of a magnetic mirror. In a tokamak these gradients are present in the poloidal direction, where the particles are trapped on so-called banana orbits. The effect of magnetic mirror is also present in the toroidal direction as the magnetic field ripple. This is caused by the finite number of toroidal field coils, albeit these gradients are not as strong as the ones in the poloidal direction, they are able to trap the particles between the coils.

1.1.2 Drifts

On the other hand, considering motion perpendicular to the direction of magnetic field, the relation (1.2) have to be multiplied by the vector of magnetic field. After minor adjustments, this leaves the equation for perpendicular component of the radius vector in the following form

$$\dot{\mathbf{R}}_\perp = \frac{\mathbf{F}_{ext} \times \mathbf{B} - \mu \nabla B \times \mathbf{B} - m\ddot{\mathbf{R}} \times \mathbf{B}}{QB^2}, \tag{1.4}$$

which is usually called the drift equation.
The first term on the right-hand side of the equation (1.4) relates to the action of an external force, e.g. the gravitational or the electric force. In the case of the electric force, the $\mathbf{E} \times \mathbf{B}$ drift occurs. This drift does not separate different charge, however it moves the whole plasma.

The second term is connected with the gradients of magnetic field perpendicular to the direction of the field. This is the case of a tokamak, where the toroidal component of magnetic field decreases with the distance from the main axis. This drift separates the particles of different charges.
The last term covers the case of non-uniform motion of the center of gyration. The acceleration can be caused by both the change of the direction (curvature drifts) and the change of the magnitude of the velocity (inertial drifts). These drifts are also accompanied by the separation of charges.[11]

1.1.3 Relativistic velocities

The energy of REs produced in tokamaks of the medium size can be tens of MeV. This is much larger kinetic energy than the rest energy of the electron (511 keV). Thus all previous consideration were quite inappropriate to deal with runaway electrons and we should rather use Hamilton equations derived from the relativistic Hamiltonian

$$H = c\sqrt{m_e^2 c^2 + (\mathbf{p} - Q\mathbf{A})^2} + Q\phi, \tag{1.5}$$

where $\mathbf{A}(t, x, y, z)$ is the vector potential of magnetic field ($\mathbf{B} = \nabla \times \mathbf{A}$) and $\phi(t, x, y, z)$ is the scalar potential ($\mathbf{E} = -\nabla\phi + \frac{\partial A}{\partial t}$).

1.2 Statistical physics and Coulomb collisions

The density of typical tokamak plasma is $n = 10^{-19} - 10^{-20}\,\mathrm{m}^{-3}$ and every particle generates its own field which affects the others, thus it is impossible to numerically solve a full scale problem through the terms of complete movement of each particle. Fortunately, this approach is not needed in the most of the cases. From the experiments we usually get the information about the properties of the whole set of particles or some important subset. According to this statement, we can leave the particle approach and move to the particle probability density function (PDF) for specific type of particles (i.e. electrons, ions, etc., will be marked generally as α) f defined as

$$dN = f^\alpha(t, \mathbf{x}, \mathbf{v}) d^3\mathbf{x} d^3\mathbf{v}. \tag{1.6}$$

The PDF determines the probability of particle position being in the specific volume element and having velocity from the specific element of velocity space. When integrated over configuration (or phase) space, this function determines the overall number of particles.[12]
Time evolution of this function can describe most of the plasma phenomena, when total time derivative is applied on the PDF, the Boltzmann transport equation

(BTE) is obtained

$$\frac{Df^{(\alpha)}}{Dt} = \frac{\partial f^{(\alpha)}}{\partial t} + \frac{\partial f^{(\alpha)}}{\partial \mathbf{x}^{(\alpha)}}\frac{d\mathbf{x}^{(\alpha)}}{dt} + \frac{\partial f^{(\alpha)}}{\partial \mathbf{v}^{(\alpha)}}\frac{d\mathbf{v}^{(\alpha)}}{dt} = \\ = \frac{\partial f^{(\alpha)}}{\partial t} + \left(\mathbf{v}^{(\alpha)} \cdot \nabla_{\mathbf{x}}\right) f^{(\alpha)} + \frac{1}{m^\alpha}\left(\mathbf{F}^{(\alpha)} \cdot \nabla_{\mathbf{v}}\right) f^{(\alpha)} = \left(\frac{\partial f^{(\alpha)}}{\partial t}\right)_{col} + \left(\frac{\partial f^{(\alpha)}}{\partial t}\right)_{s} . \tag{1.7}$$

The equation (1.7) describes the time evolution of all particles of the particular kind. The first term on the left-hand side describes the direct change of the PDE with the time, the second term is connected with the change in space caused by a flow and the last term describes the effect of forces. The first term on the right-hand side determines the change of the probability density function caused by collisions. In the case of an infinite Maxwellian plasma, this term disappears when BTEs for each kind of particles are summed together. This is not the case of tokamak plasma unfortunately. On the other hand, the second term relates to the particle sources or sinks. This must be considered in the tokamak plasma. In the special case of the Lorenz force BTE states

$$\frac{\partial f^{(\alpha)}}{\partial t} + \left(\mathbf{v}^{(\alpha)}\nabla_{\mathbf{x}}\right) f^{(\alpha)} + \frac{Q^{(\alpha)}}{m^\alpha}\left(\mathbf{E}^{(\alpha)} + \mathbf{v}^{(\alpha)} \times \mathbf{B}^{(\alpha)}\right) \cdot \nabla_{\mathbf{v}} f^{(\alpha)} = \left(\frac{\partial f^{(\alpha)}}{\partial t}\right)_{col} + \left(\frac{\partial f^{(\alpha)}}{\partial t}\right)_{s} . \tag{1.8}$$

It is important that the probability density function may be established not only for various kinds of particles, but also for some group of particles that behave very different from the bulk plasma. Such a group could be runaway electrons. The PDF of plasma containing REs is close to the Maxwellian system of thermalized electrons and runaway part expanded and shifted in the velocity space in the direction opposite the plasma current. Therefore REs distribution function could be treated separately if all the generation mechanisms are clarified.

The high temperature plasma, consisting almost exclusively of charged particles, the best approximation of collisional operator is that of Fokker-Planck or Landau. These equations deal with many small Coulomb collisions (the lower limit to the collisional parameter is determined by the complete change of the momentum vector to the perpendicular direction and the upper limit is the Debye length), where collisions are considered to be a Markov process. General Fokker-Planck equation takes the form [11, 12]

$$\begin{gathered} \frac{Df^{(\alpha)}}{Dt} = -\frac{1}{\Delta t}\nabla_{\mathbf{v}} \cdot \left(f^{(\alpha)}\langle\Delta\mathbf{v}\rangle\right) + \frac{1}{2\Delta t}\left(\nabla_{\mathbf{v}} \otimes \nabla_{\mathbf{v}}\right) : \left(f^{(\alpha)}\langle\Delta\mathbf{v} \otimes \Delta\mathbf{v}\rangle\right) \\ \langle\Delta\mathbf{v}\rangle \equiv \int \Delta\mathbf{v}\wp\, \mathrm{d}^3\left(\Delta\mathbf{v}\right) \qquad . \\ \langle\Delta\mathbf{v} \otimes \Delta\mathbf{v}\rangle \equiv \int \Delta\mathbf{v} \otimes \Delta\mathbf{v}\wp\, \mathrm{d}^3\left(\Delta\mathbf{v}\right) \end{gathered} \tag{1.9}$$

The symbol $\wp$ marks the probability of changing velocity from $\mathbf{v} - \Delta\mathbf{v}$ to $\mathbf{v}$. The first term on the RHS is dynamical friction (it is responsible for decreasing of the mean velocity of the beam particles penetrating to the plasma) and the second one cause the diffusion in the velocity space.

1.3 Primary mechanisms of RE generation

The presence of fast electrons could be a consequence of many processes. The generation of REs is usually divided into two stages. In the first stage runway seed, which is little number of energetic electrons in the plasma, is generated. Then, the number of fast electrons is multiplied by avalanche mechanism (see sec. 1.4). The runaway seed may be produced by cosmic particles, tritium decay, Compton scattering of photons on wall atoms or resonance with plasma waves. However, the most important processes are the Dreicer mechanism and the and the hot-tail mechanism that is in fact the modification of Dreicer process occurring during disruptions.

1.3.1 Dreicer mechanism

An interesting solution of the equation (1.9) for a beam of fast mono-energetic electrons penetrating into the Maxwellian plasma can be derived. This also could be the first approximation for tokamak plasma with runaway population. The second term (diffusion in the velocity space) of the RHS of the Fokker-Planck equation (FPE) is not important, because we consider the beam to be mono-energetic, so it is only slowed down. In the beginning, the first moment of the Fokker-Planck equation must be derived (by multiplying the velocity distribution function by $m\mathbf{v}$ and integrating of the FPE in the velocity space). After this adjustment, the terms in the equation must be evaluated. The space dependence may be omitted in this case and only electric force is important. The result of the derivation is equation for the velocity of beam electrons

$$m\frac{\partial v_{eb}}{\partial t} - eE = eE_D\Psi(x), \tag{1.10}$$

where E_D is Dreicer field, called critical field in the original paper [6], and $\Psi(x)$ is Chandrasekhar function

$$\Psi(x) = \frac{2}{\sqrt{\pi}x^2}\int_0^x \xi^2 \mathrm{e}^{-\xi^2} d\xi \tag{1.11}$$

of the argument

$$x = \frac{v_e}{v_0} \qquad v_0 = \sqrt{\frac{k_B T_{ep}}{m_e}}, \tag{1.12}$$

which represents the ratio of the velocity of fast electrons and the thermal velocity of plasma electrons. The thermal velocity of ions is taken as zero at this stage.

The Dreicer field is the electric field in which all electrons are accelerated and run away. The constant electric force reaches the maximum value of the collisional friction force. The Dreicer field depends on plasma electron temperature T_e and density n_e

$$E_D = \frac{n_e e^3}{4\pi\epsilon_0^2 k T_e}\ln(\Lambda) \qquad \ln(\Lambda) = \ln\left(\frac{\lambda_D}{b_0}\right), \tag{1.13}$$

where $\ln(\Lambda)$ is well-known Coulomb logarithm, defined with usage of the electron Debye length λ_D and the Landau b_0 parameter (collisional parameter of 90° scatter).

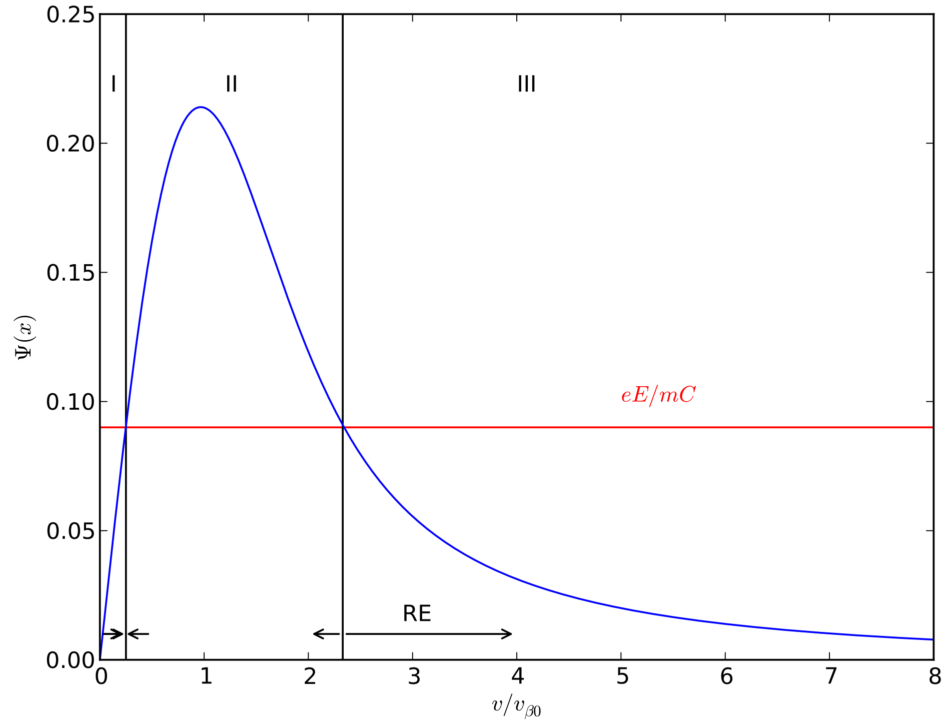

Figure 1.1: The dependence of the friction force on the velocity of plasma particles normalised to the thermal velocity. The red line is example of electric force multiplied by a constant. By comparison of these two functions it can be found whether particle of particular velocity is accelerated or slowed down. The first crossing point is stable equilibrium, the second is unstable, so all the particles in region III potentially run away.

This formula takes a slightly different form in CGS system, which is often present in theoretical papers.
With this value the most basic mechanism of RE generation is connected. The Dreicer mechanism describes accelerating of some part of electrons in the electric field stronger then the Coulombic friction force. At least some electrons are accelerated when the electric field is over so call critical field (current designation)

$$E_c = \frac{ne^3}{4\pi\epsilon_0^2 m_e c^2} \ln(\Lambda) \,. \tag{1.14}$$

The critical field multiplied by the electron charge is equal to the local minimum of the friction force, thus it is the threshold for electron acceleration in the terms of the external electric field magnitude. The friction force reaches the minimal value for the particles with their kinetic energy equal to their rest energy. Faster particles have smaller collisional frequency but they are affected by relativistic effects, so the overall slowing down force rises for higher particles with energies again.
This way of the REs generation is dominant for smaller machines with larger loop voltage and lower density. In such tokamaks the electric field overcomes the critical field at least during breakdown. Part of runaway population could be directly

released but most of them are confined. The latter are subsequently released via instabilities, during the disruptions or they can be slowed down with increasing plasma density. If there is a stable situation with electric field higher than the critical field, the number of RE grows linearly.

1.3.2 Hot-tail mechanism

So called hot-tail mechanism is slightly different from the Dreicer mechanism. It is connected mainly with disruptions. During the thermal quench, when plasma cools rapidly, fast enough electrons are not able to cool collisionally because their collisional frequency with background plasma drops very quickly. These electrons then run away, accelerated by the toroidal electric field which is increased because of the decreasing plasma current during the current quench. This way of RE generation is not connected only with the increase of electric field but it is also affected by the rapid plasma parameters change that leads to the change of the Dreicer field. In fact, the Dreicer field rises during the thermal quench (temperature is denominator in the term (1.13)), so the electric field accelerates only that fast electron population that remains almost collisionless ($\rightarrow$ "hot-tail mechanism"). Very large population of runaways can be generated this way and it can produce the REs also in the case of some particular instabilities.

1.4 Secondary mechanism of RE generation

The secondary mechanism of runaway electrons generation, that is often called the avalanche, is the most important way of production for large tokamaks and it will be crucial for ITER. This mechanism is called secondary, because it needs initial REs population which is reproduced with high growth rate. As typical loop voltage in ITER (0.1 V) should be near the value of the critical field for this machine, the avalanche will be in fact much more important than the direct Dreicer mechanism. The Avalanche is a cumulative effect of so called knock-on collisions. These are close collisions (i. e. with small impact parameter) with large amount of parallel momentum being transported. One RE electron can push several thermal electrons into the runaway region of the velocity space. These newly created runaways are able to act same way as the primary ones, so this is indeed an avalanche mechanism. If there is enough time for the avalanche to develop, the growth of the number of RE is exponential, much faster compared to the linear one in case of pure Dreicer mechanism.[19] The equation for the number of RE generated by the avalanche for the strong electric field is

$$\left(\frac{dn_r}{dt}\right)_A = \gamma_A n_r \qquad \gamma_A \approx \frac{1}{2\tau \ln \Lambda}\left(\frac{E}{E_c} - 1\right), \tag{1.15}$$

where τ is the time period defined by ratio

$$\tau = \frac{m_0 c}{eE_c}. \tag{1.16}$$

This time τ is the collisional slowing down time for the particles with the greatest probability of becoming runaway electrons.
It can be realized than even in fields just above critical field, avalanche can be very significant after long period of time.

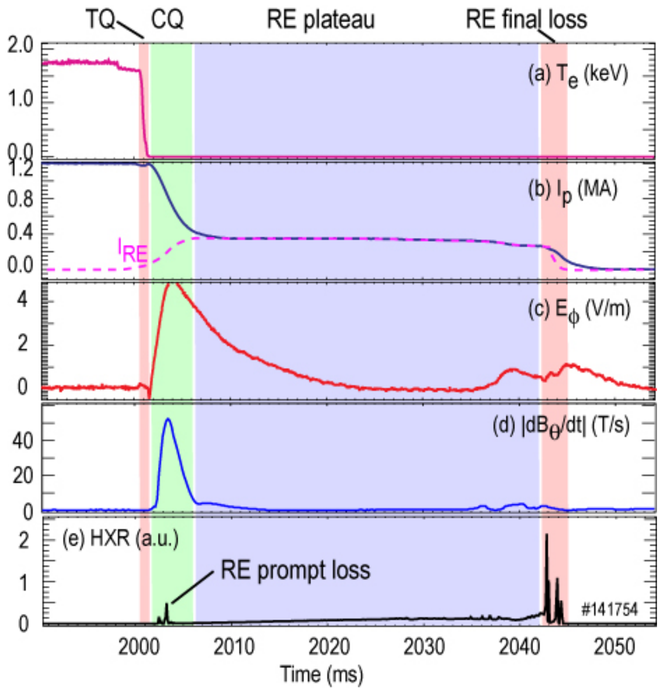

Figure 1.2: Typical evolution of important plasma parameters during the disruption with RE generation in DIII-D tokamak. The main phases described in previous text are displayed. During the TQ, hot-tail (Dreicer) process creates initial population, part of it is promptly lost, but the rest is multiplied by the avalanche. In the runaway plateau the RE carry most of the current. Finally, all RE are released. [8]

Chapter 2

Runway electrons in experiments and major trends in modelling

2.1 Detection methods

Runaway electrons are mostly detected by indirect methods. There are two types of these methods. The first kind is the detection of runway electrons presence via radiation that they generate during the motion, while the other kind measures effects of the fast electrons impacts into the tokamak wall. The only utilised method of direct detection of the fast electrons is the usage of the Cherenkov detector, which is difficult in the magnetic field of the tokamak.

2.1.1 Effects on basic plasma diagnostics

REs as a medium bearing significant part of the plasma current cause effects measurable with the traditional magnetic diagnostics. The Rogowski coil and loop voltage measurements could be used to identify the generation of runaway beam namely in the case of the disruption and subsequent hot-tail mechanism. The increase of loop voltage caused by current quench (CQ) is immediately followed by increase of plasma current which is borne by RE. This diagnostics would probably show the presence of strong avalanche mechanism too. Mirnov coils and flux loops can help with determining the runaway beam radial position, but the interpretation of the data is difficult. Namely proper plasma current density profile measurement would be extremely helpful. It is also a question, whether the equilibrium magnetic field reconstruction software (EFIT) gives relevant results in the case of the plasma with a strong runaway current. This software solves the famous Grad-Shafranov equation

$$\frac{\partial^2\Psi}{\partial z^2} + r\frac{\partial}{\partial r}\frac{1}{r}\frac{\partial\Psi}{\partial r} + \frac{\mu_0^2}{8\pi}\frac{\partial I^2}{\partial\Psi} + \mu_0 r^2\frac{\partial p}{\partial\Psi} = 0, \tag{2.1}$$

where Ψ is the poloidal magnetic flux, I is total plasma current, r and z are the cylindrical coordinates with z in the direction of the tokamak main axis and p is the pressure of the plasma. This equation is based on axisymetry and magnetohydrodynamic equilibrium. These assumptions are hardly accomplished in the pulses with

strong REs population, but we do not have sufficient replacement for this equation in more complicated situations. This is large problem as most of the modelling software relies on the equilibrium.
One of the most important parameters for the comparison with the theory is the plasma density. It can be used to determine the Dreicer field and the critical field and also the runaway production rate. Plasma electron density is usually measured with interferometers. Furthemore, the reflectometers and Thompson scattering devices are able to measure the radial density profile.

2.1.2 Radiation released by the motion of RE

There are several types of radiation according to the generation mechanism. In fact, all three types of radiation described in subsequent text may be considered braking radiation. However, for the fusion research purposes we further distinguish this mechanism according to the force or body that caused the acceleration.

- **Cyclotron emission** - The radiation caused by the gyration of electrons around magnetic field line. The frequency is usually of the order of hundreds of GHz. The frequency depends on radial position (toroidal magnetic field intensity)
$$\omega_l = l\frac{eB_0R_0}{m_eR}, \tag{2.2}$$
where l is the mode number, B_0 is the toroidal magnetic field on the magnetic axis (radial distance from the main axis R_0), R is the distance of the measurement point from main axis. The cyclotron frequency therefore drops with the distance from the main axis. The intensity of the electron cyclotron emission is usually identified with Black Body radiation
$$I(\omega) \approx \frac{\omega^2}{8\pi^3c^2}k_BT_r \qquad h\nu \ll k_BT, \tag{2.3}$$
where the temperature T_r is proportional to the component of the velocity perpendicular to the direction of magnetic field. The measured spectrum of the radiation can be transformed to the radial profile of perpedicular temperature. This method is used in the ECE diagnostics. This is as well the profile of general electron temperature if the particles have similar velocity in all directions. However, runaway electrons are usually much faster in the direction of the field. Despite this fact fast particles affect the ECE measurement because they can get trapped via knock-on collisions or they can be disturbed by instabilities. The effect of runway particles on the ECE diagnostics was measured in several tokamaks, for example in TCV, which utilises this type of the diagnostics system on both low and high field side.

- **Synchrotron radiation** The synchrotron radiation, in contrast to the cyclotron radiation, is connected with the motion parallel to the direction of the magnetic field induction vector. Regarding the high energy of runaway electrons this radiation is emitted in a very narrow cone in the direction of motion of these electrons. The theoretical formula for the total radiated power in the magnetic field of the tokamak is very complex. The spectral dependence of radiation power in the case of straight magnetic field line and $\gamma \gg 1$ is described by a formula

$$P(\lambda) = \frac{1}{\sqrt{3}} \frac{ce^2}{\epsilon_0 \lambda^3 \gamma^2} \int_{\lambda_c/\lambda}^{\mathrm{inf}} K_{5/3}(l) \mathrm{d}l, \quad (2.4)$$

where $K_n(x)$ is the modified Bessel function of a second kind.

$$\lambda_c = \frac{4\pi c m_e \gamma_{\|}}{3eB\gamma_{\|}} \qquad \gamma_{\|} = \frac{1}{\sqrt{1 - \frac{v_{\|}^2}{c^2}}}. \quad (2.5)$$

To get the more precise equation, the curvature and grad-B drifts must be taken into account.[21] Furthermore, although the single particle synchrotron radiation is not dependent on plasma temperature and density, actual radiation of runaway beam depends on these parameters. There is a huge effort to determine the runaway electron distribution from the synchrotron radiation spectrum. If this is achieved, it would be ultimate diagnostics.
The wave lengths of the synchrotron radiation for a runaway beam are usually in the infra red part of the spectrum in medium-sized machines. In bigger machines the radiation was even detected by diagnostics observing visible radiation. According to the previously mentioned facts, a fast IR camera in tangential port observing plasma in the direction opposite to the plasma current is very suitable way to measure the synchrotron radiation of the RE beam. In the case of good temporal and space resolution the position of the beam and its change can be measured. This is very important to the understanding of RE beam influence on the magnetic field, especially for some non-equilibrium magnetic reconstruction.

- **Bremsstrahlung and other radiative mechanisms** Bremsstrahlung is the radiation emitted during the Coulomb collision. As the particle is deflected and decelerated in the field of other particle the loss of the kinetic energy is compensated by emitted radiation. This happen in plasma during the collisions of electrons and ions, but it is also the main mechanism of the interaction with other states of matter, for example solid tokamak wall (see further). For relativistic electron the energy loss via bremsstrahlung is more important than the direct momentum loss during collisions (the part of the energy passed to the other particle). As the other mechanisms mentioned above, the bremsstrahlung radiation of the plasma has continuous spectrum.
  The REs may also ionize or excite the neutral or partially ionized atoms and induce the line radiation.

2.1.3 Detection of the interaction with the wall

One of the very clear proofs of the RE presence in a tokamak is the detection of high energy electromagnetic radiation with frequencies in the hard X-ray (HXR) region. This radiation is generated during the impact of the very fast electrons on the wall.

When electrons enter the very dense solid matter of the wall, they suffer strong deceleration and they emit the energy via bremsstrahlung radiation. This is in fact inelastic scattering on the nucleus. The power of the bremsstrahlung radiation depends quadratically on the atomic number Z_i. Therefore, the HXR production by this mechanism is stronger for heavier elements (metals utilised in construction of the tokamak - e. g. tungsten). The other mechanism of electron slowing down is the inelastic scattering on the bonded electrons. This leads to the excitation or ionisation of atoms and subsequent deexcitation or recombination. The steel vessel of the tokamak consist of iron and some heavier elements, so the deexcitation radiation of K shell electrons could be in the HXR region. This process is common for runaway electrons with energies less then approximately 11 MeV. For higher energies the bremsstrahlung dominates.[1] The HXR photons could directly leave the material of the wall, or they can be several times absorbed and re-emitted by the atoms of the material. Their fate depends on their energy. The photons with most energy can even trigger some nuclear reactions. The most probable type of the reaction is the production of a neutron. Neutrons produced by the interaction of the energetic photon with the nuclei are called photo-neutrons. These reactions have thresholds in the region of several MeV, often more than 10 MeV. This means that the photo-neutrons can be produced, but not in very large numbers. If the energetic photon brings enough energy that exceeds the binding energy of the nucleus, the system undergoes giant dipole resonance. This results in fission or releasing a neutron. More than one neutron could be released. Considering the materials used and proposed for the first wall, the examples of important photoneutronic reactions are $^{12}\mathrm{C}(\gamma,\mathrm{n})^{11}\mathrm{C}$ and $^{9}\mathrm{Be}(\gamma,\mathrm{n})^{8}\mathrm{Be}$.
The detection of HXR radiation is based on experiences from wide range of disciplines. Among various kinds of detector, the detectors with anorganic scintillations (NaI(Tl), CsI(Tl), ...) are used most frequently in fusion research. The scintillator converts the high energy photon into the pulse of visible light via atomic excitations. The emission and absorption spectra of the material are shifted due to the admixture (e.g. Thalium), thus the visible photons are able to leave the crystal and reach some light sensitive device. Most of these detectors use photomultiplier that need high voltage power source. However, it is possible to use semiconductor photodiode attached to the scintillator. On the other hand, semiconductor detectors of HXR could be used. These detectors are based on interaction of HXR radiation with electrons of materials like pure germanium or GeSi. The entering photon can undergo three well known processes: Photoelectric effect, Compton scattering an pair production. In the semiconductor, these processes can be detected electrically. The photoneutrons could have relatively large energy, this makes their detection harder. These neutrons are mostly detected by different kinds of scintillators, usually plastic (organic), or liquid. These materials are also sensitive to high energy photons, thus the measurement have to be carried carefully. Even tens of centimetres of high Z shielding is not enough to stop the photons released by the impact of fastest runaways and prevent the detection of gamma or HXR radiation. Unfortunately, some of the other detection options are also based on ionisation or other interaction with bonded electrons, such detectors suffer the same problem. One of the possible options is to differ the neutron and HXR pulses using complicated electronics. The other possible option is to use some nuclear reaction or transfer the

detection of neutrons to the detections of ions via proton recoil. There is a plenty of suitable nuclear reactions for thermal neutrons, but for the fast ones cross-sections of most reactions are low. However, the activation detectors and other diagnostics based on nuclear reactions were successfully tested.

2.1.4 Direct detection

The direct detection of runaway electrons is possible, however this method is very hard to implement in the harsh environment of tokamak. The speed of light in the vacuum c is the ultimate velocity, that cannot be achieved by any object with finite mass. The speed of the light inside some materials (water, transparent crystals) is considerably smaller, thus a charged particle(electron) can be faster in this environment. The movement of such particle in the dielectric materials is accompanied by emitting of the electromagnetic radiation called Cherenkov radiation. This radiation is released into the "shock cone" with axis in the direction of the particle movement (similar to the supersonic shock wave) The angle of the cone θ_c is defined by

$$\cos\theta_c = \frac{c}{nv_p}, \tag{2.6}$$

where n is the refractive index in the medium a v_p is the velocity of particle. The spectrum of this radiation is continuous and the intensity grows approximately linearly with the frequency in the visible region and peaks in the UV region. Because of this, the Cherenkov radiation has the blue colour that was observed in fission reactors.
The Cherenkov detectors are based on this principle. Fast electrons pass through the proper material (diamond, rutile - TiO_2, etc.), where they radiate by Cherenkov mechanism and this radiation is converted to electric signal and amplified by the photomultiplier. The use of this detector in the tokamak is complicated, because the detector must be close to the plasma, to secure satisfactory detection efficiency (the electrons must get to the detector before hitting the limiter or another structure). Another problem is the sensitivity of the medium to HXR photons. Rutile and some other mediums are not sensitive to photons. In case of the material sensitive to HXR, dual detector could be a solution. This means that we use one detector with magnetic shielding (magnets divert the electrons) and one without magnets. Then, it is possible to subtract the HXR signal.

2.2 Former experiments

Runaway electrons has been measured over last decades in most tokamaks and other magnetic confinement fusion devices. This phenomenon is also connected with the lightning initiation and various astrophysical issues. The most important and interesting measurements in four important tokamaks are briefly described in the following lines.

2.2.1 JET

On JET, as the largest tokamak in operation, the problem of REs earned significant experimental time. As other large machines, JET focus on the disruption generated RE. The interaction of runaway beam with carbon-fibre composite (CFC) and lately ITER-like (beryllium) plasma facing components was in the center of interest. During the experiments very powerful detection system for HXR and photo-neutrons was used. This detection system enabled the reconstruction of the RE spectra from detected HXR spectra. The new discovery was the temporal increase of the secondary maximum in HXR with increased RE plateau duration. The vertical and horizontal HXR and neutron cameras were also utilised for these measurements. The SXR tomography was able to reconstruct the RE beam spatial profile with time resolution. According to this measurements, the beam has complicated shape, usually hollow, which develops with time very quickly. An interesting result is the melioration of RE beam with vertical or horizontal movement of plasma column during CQ and subsequent stable runaway plateau. This is attributed to the influence of the changed inductance on the electric field.
The newest results with ITER-like wall shows very different behaviour of the disruptive plasma. The CQ is about 10 times slower and the temperature in the beginning is higher then in the case of CFC. This leads to lower electric fields and subsequently to lower runaway rates, which is encouraging. [17][18]

2.2.2 DIII-D

The largest American tokamak has been focusing on similar problems as JET as the disruption created runaways are one of the most important issues for ITER. The measurements of the HXR emission and basic plasma parameters after induced rapid shut-down in this tokamak have formed the understanding of the post-disruption RE beam evolution. This was described in the section 1.3.2. The HXR emission was observed either in the begging of CQ or in the end of the runaway plateau (that is stable situation with strong runaway current). The first one is the direct loss of the primary RE formed during the TQ, the second one is induced by the final loss of the very energetic RE, this is the largest danger for the wall. The results of the RE mitigation by the means of massive gas injection during runaway plateau are promising[3]. The very restricting problem is the improper function of some important diagnostics during the disruptions. For example interferometer data are corrupted because of the rapid plasma movement and changes of plasma shape and other important parameters. The prompt loss of RE is stronger in the case of diverted plasma, while for the limited plasma large runway currents in the plateau were measured. [22] This is an interesting result. With the use of the array of HXR scintillators was investigated, that the termination phase of RE plateau resembles kink instability. The DIII-D team is currently trying to find RE distribution function using various detectors, including SXR,MXR,HXR in different positions with respect to the tokamak and visual synchrotron radiation detector. [7]

2.2.3 Tore Supra

Tore Supra as a tokamak with superconducting magnets has great opportunity to study the behaviour of RE during long discharges. It even reach very long post-disruption RE plateau and study the reaction on the repetitive gas injection. During the experiments, it was proven that the original Dreicer formalism is not applicable here, as the plasma parameters evolve very rapidly and that the avalanche dominates during the later stage of disruptions. [14] Several options of RE mitigation were tested: gas injection before the disruption and during the plateau, control of the RE beam position and application of decelerating field. Conducted experiments shows different behaviour of various noble gasses in the terms of RE suppression. The lighter gasses (helium) seems to be more efficient than heavier, like argon or neon, when injected in the begging of the disruption. Helium penetrate to the plasma more quickly and the density increase is steeper. Another option - active control of RE beam barycentre - was also successfully tested. This could be an option with subsequent focusing of runaway beam into dedicated plasma facing component, a target. By this way, important components could be protected. The usage of the decelerating electric field was proved to be ineffective. [15]

2.2.4 FTU

The discharges in Frascatti Tokamak Upgrade are slightly different in comparison to previously described ones typical for larger machines. The discharges last approximately 1 s and most of the RE are generated during the current ramp-up in the beginning of the discharge. The behaviour of the discharge is similar to the Compass tokamak described in the following chapter. However, this machine is also able to produce RE during the disruptions. Lately, a three phase method of RE beam control was introduced on FTU. In the first phase of the disruption, the currents in the radial stabilisation systems are optimised. After the current quench, the Ohmic heating is turned off. Finally, during the RE plateau, the neutron and HXR emission is carefully measured and the feedback adjust the position of the runaway beam to minimize the wall damage.[2]

2.3 Important modelling tools

I have participated on 2^{nd} Runaway electrons modelling workshop, which took place at Chalmers University in Gothenburg, Sweden. During this meeting most of the attitudes towards the modelling of RE and its results were presented.

2.3.1 CLQ3D

Collisional/QuasiLinear 3D code is the relativistic model that solves the Bounce-averaged Fokker-Planck equation in the 3 and 1/2 dimensions (parallel and perpendicular velocity, radius and implicit poloidal angle). The code was originally developed for the RF heating ray-tracing and it can find solutions for electron and ion distribution, time-dependent and time-independent. For the use in RE modelling, the code was enriched by the "knock-on" collision operator. The code is written in Fortran.

2.3.2 ARENA

Analysis of Runaway Electrons by Numerical Algorithms is another solver of bounced kinetic equation. This model works in 1+2 dimensions (1 space/2 velocity). The model combines the solution of the kinetic equation by the Monte-Carlo methods (particle code) with application of finite elements to solve the electric field diffusion.[20]

2.3.3 LUKE

LUKE is very complex RE dynamics code utilised in Integral tokamak modelling, which is an effort to completely cover the behaviour of plasma in the tokamak. It is a 3D guiding center code that solves the electron kinetic equation. It contains Fokker-Planck and knock-on (close coll.) collisional operators, RF heating, Synchrotron emission and other operators that affect the probability density function of electrons. This software may be used in the study of fast electron dynamics and also in predictive or interpretative mode for comparisons with experimental data. It is connected with the databases of many tokamaks (JET, TCV, EAST, etc.). The Compass database was connected recently. This model is continuously developing.[5]

2.3.4 GO

GO is fast 1D fluid model of cylindrical plasma that is specially designed to describe the plasma with the disruption generated runaway electrons. It contains all the most important processes including electric field diffusion and radiation to solve the energy balance of electrons, ions and impurities.

2.3.5 CODE

COllisional Dynamics of Electrons is very compact and fast model of basic runaway dynamics. Its purpose is the fast computation of RE distribution and synchrotron emision of plasma with given parameters. Such fast software may find application in the feedback systems of tokamak.[13]

Chapter 3

Experiments on COMPASS and GOLEM tokamaks

3.1 COMPASS data

COMPASS is smaller and flexible machine operated by the Instituted of Plasma Physics, Academy of Science, Czech Republic since 2006. The usual shape of the plasma is close to the shape proposed for ITER. Due to this resemblance, many ITER-relevant project are conducted on this machine. Most of them are connected with the edge plasma diagnostics and plasma-wall interaction. Despite this, the machine is also able to create the conditions for RE experiments. As a small machine with relatively high loop voltage the RE are usually created during the start-up phase, they are also driven or released by some instabilities. It is not excluded that also disruption created RE could be produced. Due to the shorter time scale (in comparison with large machines), COMPASS is not very suitable to disruption RE experiments, yet can bring the interesting information in the terms of scaling. During the years of operation, the presence of RE was detected many times by the HXR scintillation located in the north direction, 3 metres from the tokamak.

3.1.1 Coincidence of ST crash and RE bursts

The saw-teeth instability (ST) is well known as it was observed in many tokamaks. However the exact mechanism was not yet uncovered. This instability manifests with periodical signal of saw-teeth shape in measured by the SXR diagnostics. The signal of SXR is proportional to the plasma temperature. Similar periodicity is observed in density signal measured by the interferometer. The SXR channels that observe the plasma center have inverse signal to the channels that measure the plasma edge. This means that the temperature in the center drops suddenly, while in the edge it rises. This is interpreted as the symptom of the magnetic reconnection. The hot plasma center is thrown to the colder regions while the topology of magnetic field lines is changed. The ST is probably triggered by the internal kink (the magnetohydrodynamic instability that twists the plasma column). The evidence can be seen in

the data (figure 3.1). This instability is often observed in COMPASS during pulses with elongated or triangular plasma. The size of the ST is generally amplified by the neutral beam and other auxiliary heating devices.
During a number of shots, periodic, unusually high HXR peaks were observed immediately after the ST crash. Similar signal was measured in TCV and other machines. The interpretation of this phenomena is ambiguous.

Possible explanations

The first possible explanation is the acceleration of the electrons in the electric field created by the rapid change of the magnetic field according to Maxwell equation

$$\frac{\partial \mathbf{B}}{\partial t} = -\nabla \times \mathbf{E}. \tag{3.1}$$

This process is well known from the universe, e. g. charged particles are accelerated by this process in the magneto tail of Earth and reach very high energies. However, on the scale (quick, very localised in space) the phenomena is observed in the tokamak, the electrons could be hardly accelerated to measured energies. However the local reconnection field could be up to 1000 V/m
The other explanation describes the coincidence as a sudden leak of confined RE. The well confined fast electrons are thrown from the center of the plasma due to magnetic reconnection. Some of them may get to the banana orbits and drift to the limiter. This theory predicts that the impact of RE burst is delayed with respect to the ST crash for about 200 μs **??**.
Both processes may be involved and further supported by some modification of the hot-tail mechanism (the ST is often called "internal disruption"). However in current state of research, it seems the process of de-confinement of RE is dominant.

Pulses with ST and possible correlations

The phenomenon can be observed in signals measured during numerous shots (more than hundred), but usually it is hard to distinguish the peaks connected with ST and peaks caused by common RE losses. During several shots, there were also problems with diagnostics, e.g. malfunction of the interferometer or saturation of SXR measurement. The effect was first noticed in signals of pulses #4413-4425. These were D-shape, H-mode experiments with neutral beam heating and relatively high density. Some of these experiments have ended by disruptions. The evolution of the effect during the pulse #4420 is in Fig. 3.3. The peaks disappear despite the continuing ST. This behaviour seems to be independent on the density. The

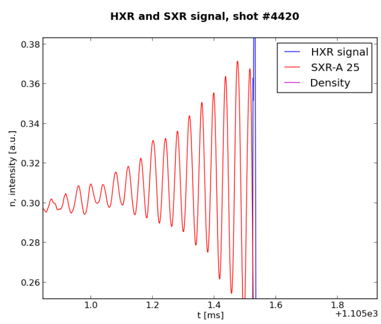

Figure 3.1: The situation before the ST crash enlarged, giant kink instability as the precursor of ST crash can be distinguished in periodic behaviour of SXR signal.

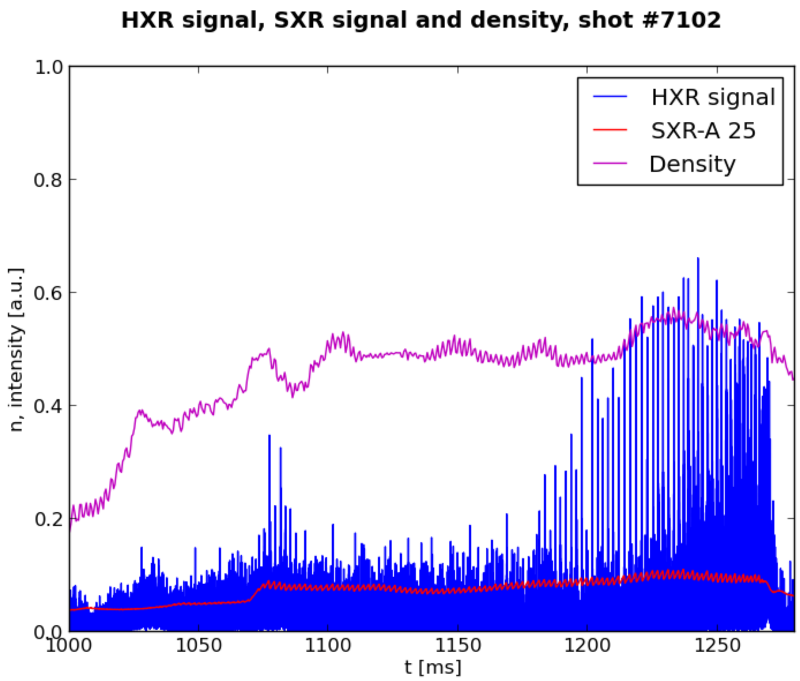

Figure 3.2: The coincidence of the saw-teeth instability in the SXR data (channel 25, camera A) with HXR peaks, corrected density displayed, no neutral beam injection during this shot.

ST is very large as the significant part of neutral
beam power heats the electron population. In this situation the HXR peaks are huge and well defined. The detail of the precursor to the ST, the internal kink is in the Fig.3.1.
On the contrary this phenomenon was present also in experiments without NBI, e. g. #7101,7102 (Fig.3.2). These were again D-shape experiments, but without the auxiliary heating. The saw-teeth was very stable in these experiments, but quite small (no aux. heating, lower temperature). Several peaks occur in the beginning of the ST followed by minor drop of density, then the ST continues without significant HXR peaks and in the end the ST-connected peaks appear again very clearly. The reason for the interruption is unknown. It was recorded that RE can be strongly influenced by any perturbation of magnetic or electric field or small obstacle (e.g. entering of the reciprocating probe, resonant magnetic perturbations (RMP), etc.). This may be the case.
It seems that the HXR peaks are caused rather by release of RE originating from the breakdown than sudden acceleration during magnetic reconnection. According to the Figure 3.4, the RE could be hardly created in the flat-top phase of the discharge, namely in the case of #7102. On the other hand the break-down field is sufficient. However, the situation during the break down is much more complex, e. g. the electrons in weakly ionised gas suffer different type of friction force. The acceleration of the RE by standard Dreicer process in between the ST crashes could be excluded from the list of possible explanations. The reconnection region is quite

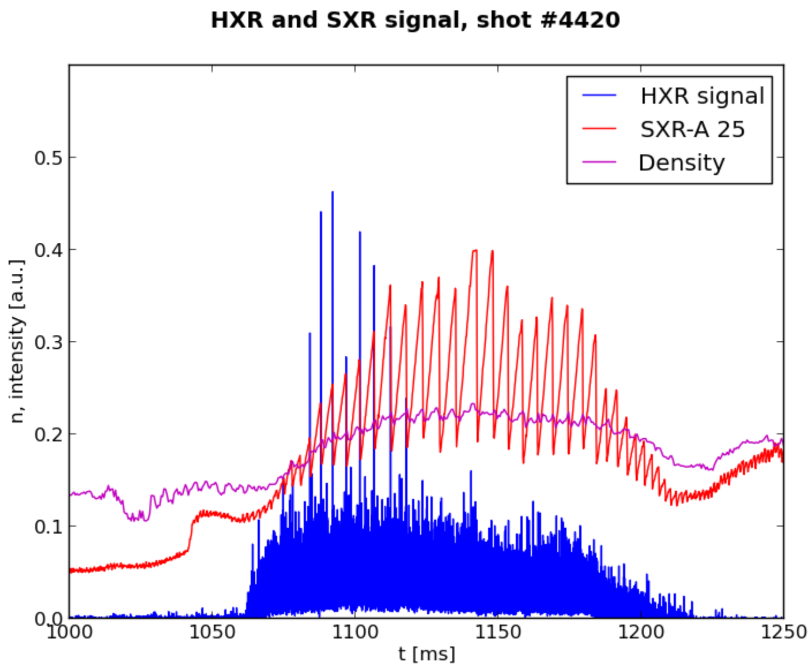

Figure 3.3: The coincidence of the saw-teeth instability in the SXR data (channel 25, camera A) with HXR peaks, corrected density displayed, both neutral beams worked (NBI1: 1080-1140 ms + 1155-1200 ms, NBI2: 1060-1180 ms)

small in comparison to the astrophysical plasma. This means that the electrons have to go through the region many times (several hundreds or thousands) to gain the measured energies in the field created by the change of the magnetic field. The delay of the HXR peak after the ST crash is in the order of tens of μs. This information could help with the discrimination of possible explanations, albeit the theory of the reconnection is not complete and several models with different characteristic times were introduced [11]. No significant correlation was found between the parameters of the ST (the size of the fall or period) and the size of the HXR peaks. The measuring of HXR is indirect method of RE detection and it is affected by many factors. A direct method of electron measurements inside the vacuum chamber would be much more suitable for this purpose. Such detector could help to solve the question of the origin of these RE. The correlation graphs are in Figures 3.5 and 3.6. The former is the correlation of the size of the ST crash. A positive correlation would be reasonable in both mechanisms (reconnection acceleration and release of confined electrons). The latter is the correlation of the ST period and the size of HXR peaks. The size of the ST crash and the period are strongly bonded, so their correlation with the number and energy of released runaways (= intensity of HXR) would be similar. If it would be possible to separate the dependence on the size of the crash and the dependence on the period, positive correlation with period would suggest that the REs are accelerated in between the ST crashes. This is almost excluded by the high critical field value mentioned above.

This topic definitely needs further study. It will be examined during one of the upcoming dedicated campaigns on COMPASS. The first dedicated one was focused

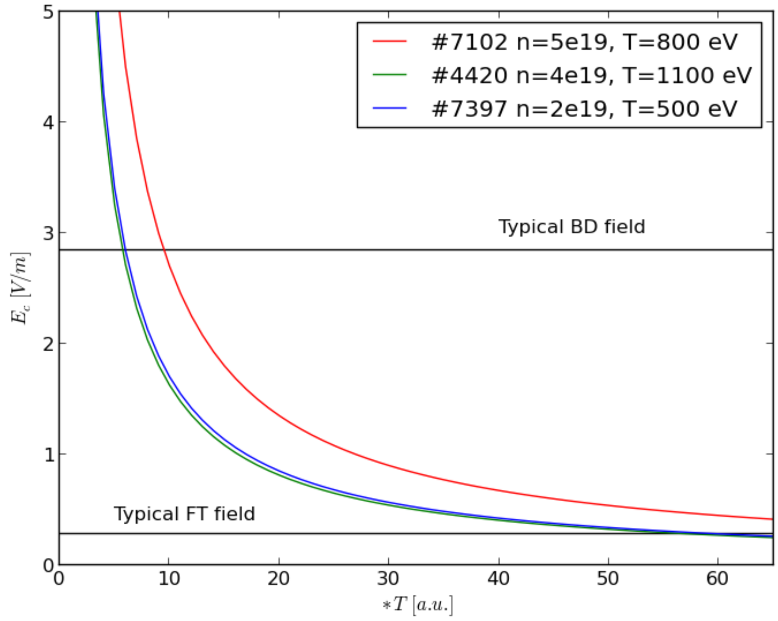

Figure 3.4: Critical fields of three different discharges as a function of the energy of electrons (in the terms of multiplications of temperature). Comparison with typical COMPASS breakdown and flat top field. If the curve is under the line, the particles are accelerated. Pulses #7102 and #4420 were describe in the text, pulse #7397 is the typical experiment of the first dedicated campaign, notice the low density. Especially the presence of the RE burst in pulse #7102 is very interesting according to this comparison.

on the circular plasma discharges. In circular plasmas, ST is rarely observed.
The phenomenon is not in the focus of large machines as RE created during the disruptions are more dangerous and could be the largest threat for ITER. The HXR diagnostics in these machines has often lower time resolution as it is focused rather on space resolution and attempts to reconstruct the probability density function of RE. On the other hand sufficient knowledge of the ST-generated RE may also help to better understand the disruption created RE.

3.2 Dedicated COMPASS campaign

The COMPASS team was recently charged with project dedicated to the runaway electrons, benchmarking of the models and the development of the RE suppression methods. In the case of some positive results the project will last 5 years. The first dedicated campaign was held in May.

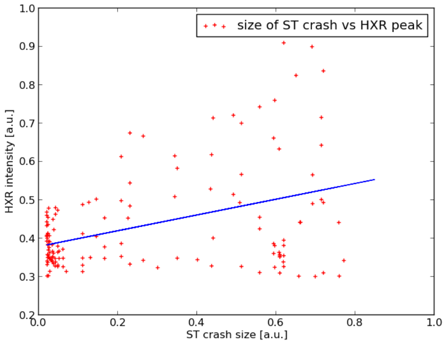

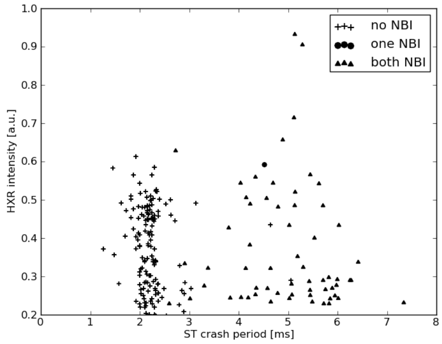

Figure 3.5: The correlation of the size of the ST crash and the size of the subsequent HXR peak. Slightly increasing linear trend may be observed. In case of direct measurement of RE release this correlation would be probably stronger.

Figure 3.6: The correlation of the ST period with the size of HXR peaks with respect to the neutral beam heating. It is obvious that the period prolongs with increasing NBI power. However, the desired correlation is very weak if any.

3.2.1 Detectors

HXR

For these experiments, new scintillation detectors with photo-diode were ordered. This modern modification removes the strong requirement of the detector for the excellent high voltage (HV) power source. As the photomultiplier is replaced by the super-sensitive photo-diode, the detector could be powered by 12 V power source or by battery. Unfortunately only one of these detectors was already in place and it had to be adjusted to the better time resolution.

As a replacement, 3 NaI(Tl) 2" scintillation detectors with the photomultiplier in positive polarity regime were borrowed from the Department of Dosimetry, FNSPE CTU. The native HXR detector at COMPASS is almost of the same type, albeit currently in the negative polarity regime. These borrowed detectors were older, but sufficient for the purposed measurements. 2 HV power sources (PS) were also borrowed and the last detector was powered by an old source form IPP. As the permanent HXR detector is near the north wall of the tokamak hall, the borrowed detectors were placed in the middle of all remaining walls, approximately 3 metres above the ground.

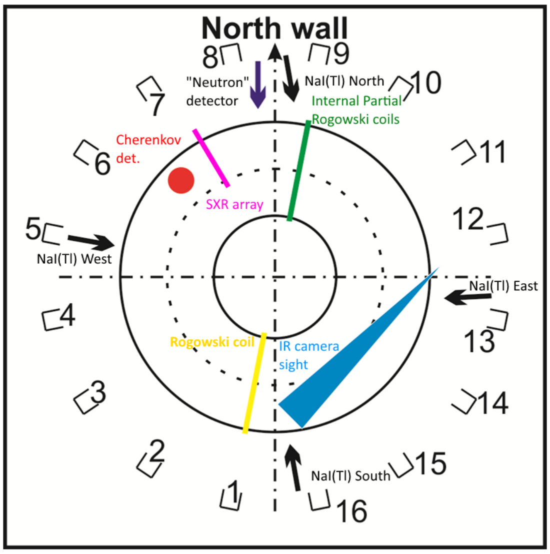

Figure 3.7: The upper view of tokamak COMPASS with marked positions of the diagnostics that is affected by RE.

Insulation transformers were used to connect the sources to power, however in the first measurements strong oscillation at 50 Hz were observed. In the end the insulation transformer was used only with the old PS from IPP. However, there was still very strong noise on the three new channels. After the experiments it was found that it was caused by the common grounding (all BNC cables were connected to the same reduction box with Ethernet output and connected to data acquisition system). The measurements of the noise in various configurations are attached.

IR camera and Cherenkov detector

In order to detect the synchrotron emission, IR camera was placed in the tangential port, observing the plasma in the standard direction of the plasma current. The other IR camera was in the radial port, focused on the inner limiter where the fraction of the RE beam energy was deposited. All important diagnostic systems are displayed in figure 3.7. The Cherenkov detector was prepared by Polish colleagues from National Centre for Nuclear Research. The new measuring head was equipped with diamond radiator. Although this solution should be very sensitive, there was rarely clear signal on the detector during this campaign.

"Neutron" detector

Another scintillation detector is placed north to the tokamak on the floor and shielded by 10 cm of lead. This was proposed as a neutron detector. However, we have found during the measurements that the shielding of HXR is not sufficient. After placing neutron stopper (plastic balls) around the lead shielded detector, there was still strong signal partially coincident with other HXR detectors. This means that we do not have independent measurement of photo-neutrons.

3.2.2 Conducted experiments

As was mentioned before, this first campaign was focused on basic properties of RE in tokamak COMPASS. Therefore, the production of RE in circular plasma was measured as the basic parameters were changed in between the shots. Conducted experiments:

- Density scan
- Position scan (radial, vertical)
- Incomplete I_p scan
- Incomplete shape scan
- Rough B_t scan

- Reversed I_p, a few disruptions, NBI, gas puffs

Along with the RE campaign, the Resonance magnetic perturbation (RMP) campaign has taken place. The RMP coils are one of the options considered for the RE suppression. This means that some very interesting data from our point of view were measured as a by-product of these experiments.

3.2.3 Preliminary results

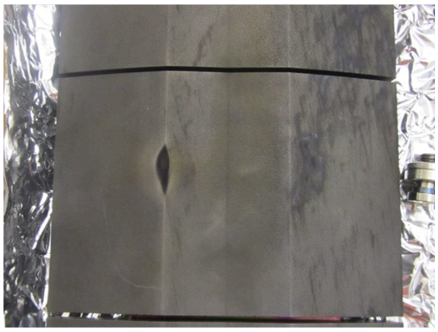

Figure 3.8: The "double roof" high field side limiter after the campain, The damage caused by the RE beam is obvious

The measured data has not yet been fully analysed, only some of the most interesting preliminary results are listed here. The devastating power of RE beam is illustrated in the fig 3.8. During some pulses a periodic HXR signal was measured either in the flat-top or during the ramp-down. The period is slightly above one millisecond (it is equal to the period of very small ST instability) and it seems that there is some phase shift between the detectors it the toroidal direction. However the shift is smaller than the FWHM of the peaks so it is hard to say whether this is caused by the different time of detection or by the properties of the detectors. Quantitative analysis of this effect is planned. During the circular shots, no ST was observed in SXR data, albeit during the parallel RMP campaign similar signal coincident with small ST was observed. The periodic release may be caused by some internal MHD activity that is not strong enough to trigger ST or the temperature drop is not large enough to be measured by the SXR diodes. The idea of the correlation of RE release with MHD activity is supported by same patterns in MHD and HXR spectrograms. The release of the electrons was sometimes so strong that it affected even the SXR diagnostic (Figure 3.9). During the periodic release also the loop voltage and I_p change periodically, albeit in quite different pattern. The RMPs strongly affect this phenomenon.
The data from the IR camera situated in the tangential port may show some evidence of RE synchrotron radiation. A well defined radiating circle was recorded during several pulses. In the same configuration with reversed current there was no such subject. However it is early to claim that we have observed synchrotron radiation. The special IR spectrometer has measured no signal.
The measured data will undergo further analysis in next months in order to specify the focus of the upcoming second campaign (November).

3.3 GOLEM data

Tokamak GOLEM is the oldest working tokamak in the world, now located at the Faculty of Nuclear Sciences and Physical Engineering. The plasma volume and the

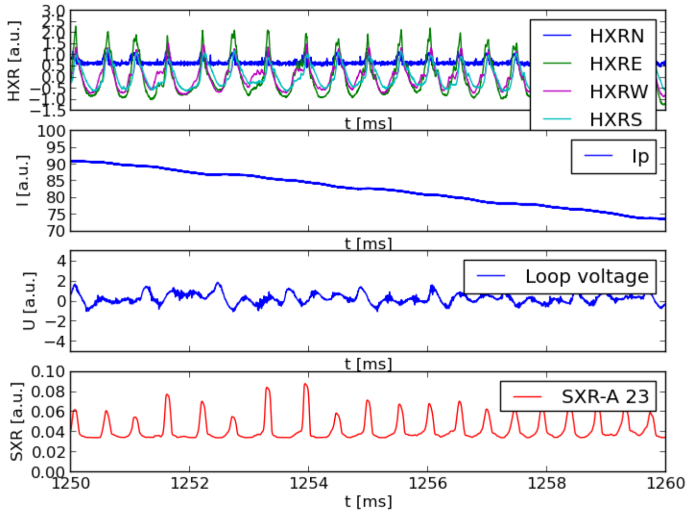

Figure 3.9: The signal of four HXR detectors, loop voltage, plasma current and SXR signal during periodical release of runways. (COMPASS)

temperature is quite small with respect to current devices. The low temperature and density of plasma with relatively high impurity presence and very high loop voltage is very suitable for the creation of RE. Unfortunately the machine is currently not equipped with density diagnostics. The only possible way to estimate the density is to use the value of pressure in the tokamak chamber before the discharge. This is very inaccurate as the ionisation of the gas may not be complete (typical temperature $T_e = 15\,\mathrm{eV}$ vs. ionisation potential for hydrogen $13,6\,\mathrm{eV}$) and we have no information about wall adsorption, leaks, impurities etc. The installation of the interferometer is planed. For the typical temperature 15 eV and density $2 \cdot 10^{18}\,\mathrm{m}^3$ (rough estimation) the Dreicer field is 45 V/m and the critical field is as low as several mV/m. In comparison to the typical loop voltage of 6 V, this means quite strong RE production indeed.

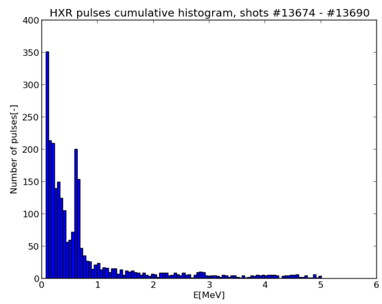

Figure 3.10: The histogram of HXR pulses in energy before the deconvolution of peaks, full absorbtion peak of Cs 137 at 662 keV (used for calibration) is obvious.(GOLEM)

3.3.1 HXR measurements

During numerous shots the HXR scintillation detector (2" NaI(Tl) with photomultiplier) was placed near the tokamak. Unfortunately the HXR intensity in the tokamak room is very high and with current amplifying level, the signal is often saturated. This is a serious problem for spectrum analysis, however different kind of analysis is

possible. Despite the above mentioned difficulties, we can make a histogram of HXR pulses in energies 3.10. The tail of the histogram is deformed by the coincidence of HXR pulses, but the low energy part is close to reality. Therefore, the energy of RE in this tokamak certainly reach at least 1 MeV.
During previous measurements on GOLEM was measured that the overall intensity of HXR signal decreases linearly with increasing pressure. This seems to be logical, albeit the overall intensity of HXR signal is very ambiguously defined quantity (namely in the case of saturated signal) and the pressure measurement do not properly reflect the electron density. The HXR signal is very dependent on the size of

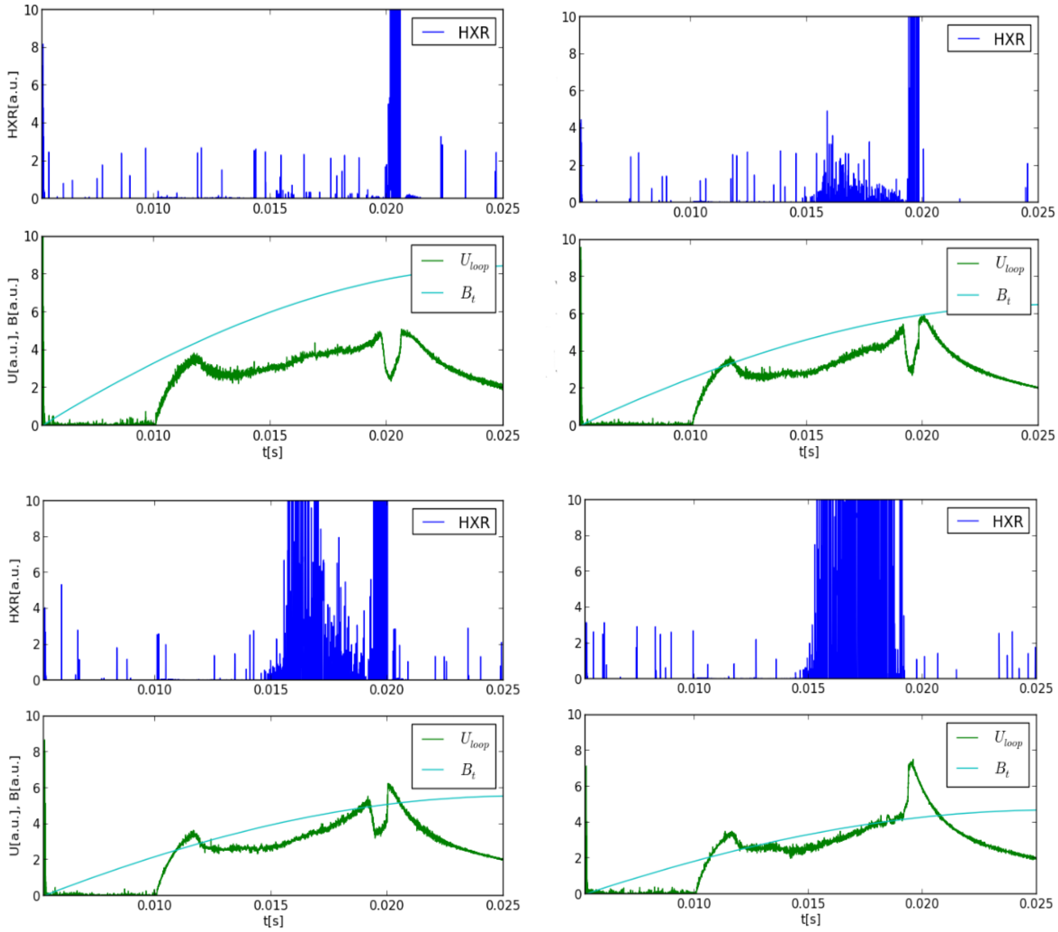

Figure 3.11: The change of the HXR emission with decreasing toroidal magnetic field magnitude. Pressure and maximum value of primary windings voltage were kept constant.(GOLEM)

the toroidal field. This can be observed in figure 3.11. During these four shots the pressure of the working gas and the voltage in the capacitors supplying the electric field was set constant. With the reducing magnetic field the nature of the of the RE loss changes from sudden release right before the end to continuous losses during the whole second half of the discharge. This is definitely connected with confinement of the fast particles. The situation is well illustrated by the figure 3.12. The graph de-

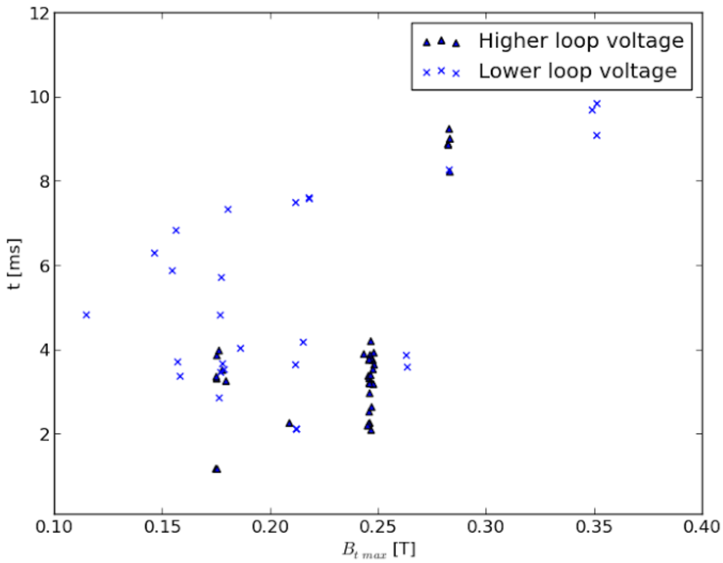

Figure 3.12: The delay of the beginning of HXR emission with respect to the breakdown as a function of the toroidal magnetic field, the behaviour of the signal is different for lower and higher fields. (GOLEM)

scribes the relation between the toroidal magnetic field magnitude and the delay of the massive HXR emission with respect to the time of the breakdown. It is apparent that there are 2 regimes. In the first one, the field is not sufficient to confine the runaways that gained enough energy, thus they leave the plasma volume. The time this happens should be dependent on the electric field magnitude. In the second regime, the RE are confined within higher field to the end of the discharge and their release is sudden, triggered by some instability (it could be the vertical displacement together with some low temperature equivalent of the disruption hot-tail process - see further). The two different types of the discharge (continuous versus sudden release of RE) can be distinguished even by the fast camera images. It is obvious that the plasma is not vertically stabilised and travels upwards. The images of the discharges with "secondary breakdown" contain typical dark region at the moment before the secondary current ramp-up (figure 3.14). It seems that the discharge is almost over, however the strongly accelerated RE electrons, that bear the most of the current are able to re-ionize the plasma for a short period (so far the vacuum loop voltage is sufficient), either directly or by the secondary emission after the impact. No such dark region is observed in the images of discharges without final HXR emission - Figure 3.13. Furthermore, it seems that the steeper the secondary ramp-up is, the more obvious is the "clinical death" of the plasma.
Similar phenomena may be observed repeatedly in the data of the discharge with vertical stabilisation tests. The plasma was repeatedly affected by the fast change of the vertical stabilisation field and the discharge almost terminated. However, the subsequent recreation of plasma was accompanied by strong HXR emission. The process looks similar to the final loss mentioned previously.

The independent diagnostics of density would help to identify the undergoing processes. It would be possible to compare the measured data with theory (critical fields, acceleration times) more efficiently. The installation of the interferometer is prepared for this year. Although the plasma of tokamak GOLEM is very different from the plasma of large machines the study of the RE generation mechanism may help with understanding of the problem on the small-scale.

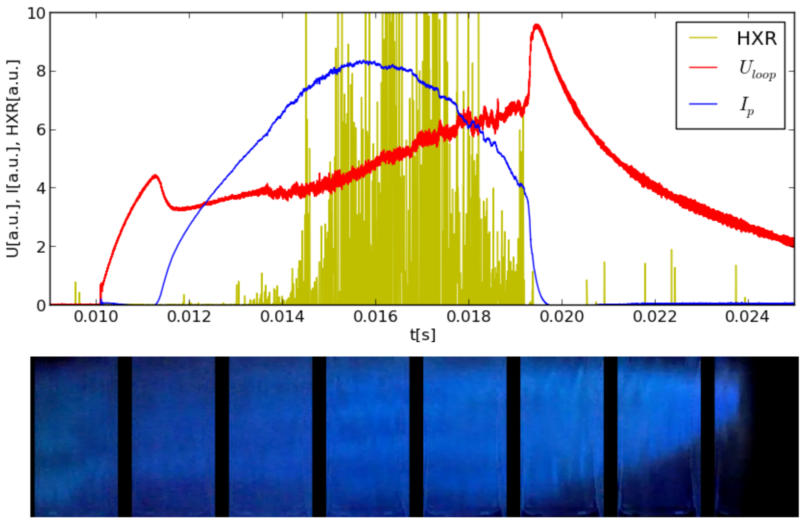

Figure 3.13: The discharge #14591, without final loss of HXR

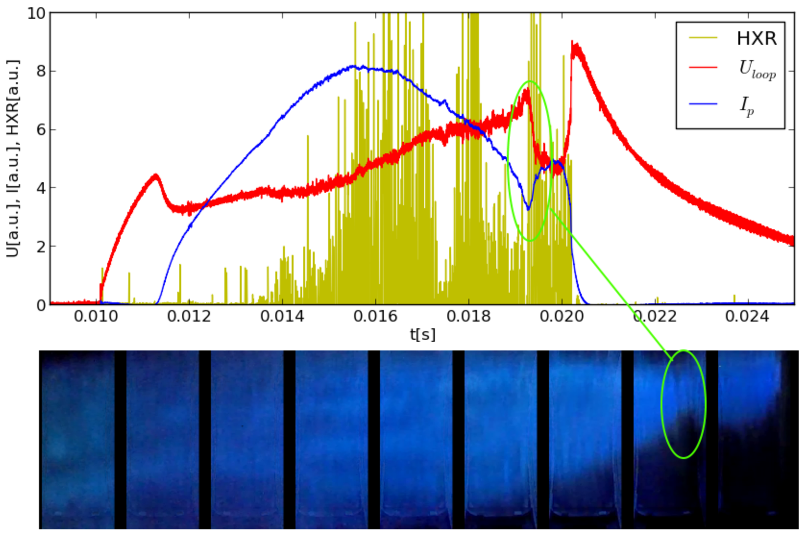

Figure 3.14: The discharge #14592, minor final loss of HXR, some evidence of plasma collumn interruption in the fast camera image.

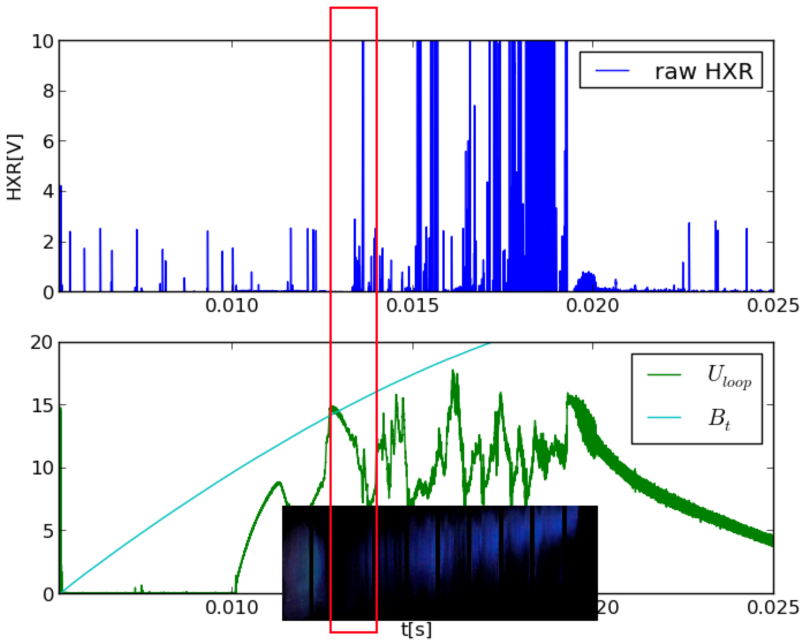

Figure 3.15: The discharge #14580, vertical stabilisation tests, repetitive interuptions of plasma apparent in the image accompanied by the HXR emission.

Summary and outlook

This work was dedicated to runaway electrons as one of the most dangerous and interesting phenomenon in the present tokamak research. These fast charged particles represent serious danger for the operation of large tokamaks, including ITER. Before the first plasma in this ultimate machine, the mechanisms of the RE creation have to be fully understood and the techniques to minimize the damage must be developed.

The first chapter is very brief introduction into the physics connected with RE. The generation processes are shortly described. The second chapter is focused on the detection techniques, important former experiments and the most important tools in modelling. In the third chapter, the results of experiments conducted on both Czech tokamaks are presented. The first part of this chapter is focused on the connection between the saw-teeth instability and the periodic release of runaway electrons. The second part describes the first campaign dedicated to the runaways on Compass. During these experiments, the periodic behaviour of HXR signal was observed again, although without apparent ST instability. Later was found that this behaviour is caused by Parail-Pogutse instability. In the last part, some interesting results from tokamak Golem are described. The crucial role in the RE beam confinement and subsequent HXR detection plays the magnitude of the toroidal magnetic field.

3.4 Further plans

3.4.1 Golem

- Revision of scripts connected with runaways, optimization of the deconvolution algorithm
- Find out how to avoid the saturation of the HXR signal, installation of the new HXR probe
- Help with installation of the interferometer
- Feasibility studies of timepix diagnostic (semiconductor detector used in particle physics) for the detection of runaway electrons in the tokamak
- Data analysis with respect to the new diagnostics

3.4.2 Compass

- Further analysis of HXR and other relevant signals from the first dedicated campaign
- Help with preparation of new CdTe - photo-diode detectors
- Participation on the second dedicated campaign

3.4.3 Theory and modelling

- Hopefully participation in some basic modelling work (CODE?)

References

[1] BUSHBERG, T. J.; SEIBERT, J. A.; LEILDHOLDT, E. M.; BOONE, J. M. *The Essential Physics of Medical Imaging.* Lippincott Williams & Wilkins, 2011.

[2] CARNEVALE, D. *A first approach to runaway electron control in FTU.* Fusion Engineering and Design 88 1109-1112, 2013.

[3] COMMEAUX, N., et al. *Novel Rapid Shutdown Strategies or Runaway Electron Suppression in DIII-D* Nucl. Fusion 51 103001, 2011.

[4] CONNOR, J.W.; HASTIE, R.J. *Relativistic limitations on runaway electrons.* Nucl. Fusion 15, 1975.

[5] DECKER, J.; PEYSSON, Y.; BRIZARD, A. J.; F.-X. Duthoit. *Orbit-averaged guiding-center Fokker–Planck operator for numerical applications* Physics of Plasmas 17 112513, 2010.

[6] DREICER, H. *Electron and ion runaway in a fully ionized gas, I*.* Physical Review, vol. 115, 1959.

[7] HOLMANN, E.M., et al. *Measurement of RE f(E) evolution following MGI into RE plateau* REM Workshop, Gothenburg, 2014.

[8] HOLMANN, E.M., et al. *Control and dissipation of runaway electron beams created during rapid shutdown experiments in DIII-D* Nucl. Fusion 53 083004, 2013.

[9] LONGWEN, Y.; BINGREN, S.; YIMING, J. *Sawtooth-induced loss of runaway electrons in tokamaks.* Plasma physics and fusion technology, Vol. 33, Iss. 18, 2001.

[10] KOCMANOVÁ, L. *Runaway electrons in the tokamak and their detection.* Master thesis, FJFI ČVUT v Praze, 2012. `http://fttf.fjfi.cvut.cz/StPrace/Diplomky/2012/KocmanovaLenka.pdf` [3.9.2014]

[11] KULHÁNEK, P. *Úvod do teorie plazmatu.* AGA, Praha, 2013.

[12] KRACÍK, J.; ŠESTÁK, B.; AUBRECHT, L. *Základy klasické a kvantové fyziky plazmatu.* Academia, Praha, 1974.

[13] LANDREMAN, M.; STAHL, A.; FÜLOP, T. *Numerical calculation of the runaway electron distribution function and associated synchrotron emission.* Computer Physics communications Vol. 185, Is. 3, 2014.

[14] MARTIN, G. *Runaway electrons from Tore-Supra to ITER* Proc. 25th EPS Conf. on Controlled Fusion and Plasma Physics, Praha, 1998, pp. 651–654

[15] SAINT-LAURENT, F. *Disruption and runaways electron mitigation studies on Tore Supra* EXS, 2010, 2: 16.

[16] PAPP, G. *The role of magnetic perturbations in runaway electron and sawtooth dynamics.* Doctoral thesis. Chalmers university, Gothenburg, 2013.

[17] PLYUSNIN, V.V., et al. *Latest progress in studies of runaway electrons in JET.* 24th IAEA Fusion Energy Conference, San Diego, 2012.

[18] PLYUSNIN, V.V., et al. *Study of Runaway Electron Generation During Major Disruptions in JET.* Nuclear Fusion, 2006, 46.2: 277-284.

[19] ROSENBLUTH, M.N.; PUTVINSKI, S.V. *Theory for avalanche of runway electrons in tokamaks.* Nucl. Fusion 37, 1997.

[20] RYDÉN, J. *Monte carlo simulation of runaway electrons.* Master thesis, Chalmers University of Technology, 2013. `http://ft.nephy.chalmers.se/JakobRyden_thesis_final.pdf` [3.9.2014]

[21] STAHL, A.; LANDREMAN, M.; PAPP, G.; HOLLMANN, E.; FÜLÖP, T. *Synchrotron radiation from a runaway electron distribution.* Physics of Plasmas 20, 2013.

[22] TRONCHIN-JAMES, A. N. *Investigations of runaway electron generation, transport, and stability in the DIII-D tokamak.* Doctoral thesis. University of California, San Diego, 2013.

[23] ÚLEHLA, I.; SUK, M.; TRKA, Z. *Atomy, jádra, částice.* Academia, Praha, 1990.

[24] WESSON, J. *Tokamaks.* Oxford University Press, New York, 2004.

Appendix

Appendix A

Additional cloud storage content

Every source (unpublished papers, presentations), working files (e.g. the values of the noise of borrowed detectors) and scripts created for the purposes of this work may be placed here if you ask me.

`https://drive.google.com/folderview?id=0Bz7wTD2cnvNHSEFTNTZTXzZReFU&usp=sharing`